PROGRESS IN ENGINEERING APPLICATION AND TECHNOLOGY
e-ISSN: 2773-5303

PEAT

Vol. 7 No. 1 (2026) 597-610
https://publisher.uthm.edu.my/periodicals/index.php/peat

Development of Activated Carbon from Lemang bamboo (Schizostachyum brachycladum) to Absorb Synthetic Pollutant Methylene Blue

Muhammad Naim Najmie Sokarno[1], Rama Yusvana[1*]

[1] *Faculty of Engineering Technology, Universiti Tun Hussein Onn Malaysia*
UTHM Kampus Pagoh, KM1 Jalan Panchor, 84600 Muar, Johor, MALAYSIA

*Corresponding Author: rama@uthm.edu.my
DOI: https://doi.org/10.30880/peat.2026.07.01.068

Article Info

Received: 12 January 2026
Accepted: 20 February 2026
Available online: 25 May 2026

Keywords

Activated Carbon, Schizostacyum Brachycladum, Methylene Blue, Adsorption, Wastewater treatment, Physical Activation, Superheated Steam

Abstract

This paper examines the creation of sustainable activated carbon from Schizostachyum brachycladum (Lemang bamboo) as an eco-friendly adsorbent for the removal of pollutants from wastewater using Methylene Blue as synthetic pollutant. To address the environmentally associated problems of conventional coal-based activated carbon, this study employed a physical activation process using superheated steam at 750°C for the preparation of the adsorbent. The study extensively analysed the physicochemical properties of the processed AC through Scanning Electron Microscopy (SEM), Fourier-Transform Infrared (FTIR) spectroscopy, and X-ray Diffraction (XRD) analyses to examine the surface properties and functional groups. Moreover, this study examined the effects of the particle size (ranging 1-3 mm) of the adsorbent on the efficiency of the process and the regenerability of the adsorbent through temperature treatments in several cycles. The experiment showed that the process obeyed the Langmuir isothermal equation with a very high correlation coefficient (R^2 = 0.9988), indicating monolayer adsorption, while it obeyed pseudo-second-order kinetics. Finally, this research work proves that Lemang bamboo is an ideal, affordable, and sustainable source for the preparation of high-quality activated carbon with promising applications for sustainable wastewater treatments.

1. Introduction

Activated carbon has established itself as an essential material for wastewater treatment, drinking water purification, and exhaust filtration. Due to its versatility and tightening global environmental restrictions, the demand for activated carbon is anticipated to rise significantly. While commercial activated carbon is traditionally derived from non-renewable precursors like coal, recent research has pivoted towards biomass alternatives. Studies have successfully utilised diverse precursors, including waste palm trunk, fruit residues, and coconut leaf [1]. Among these, bamboo stands out as a renewable, low-cost resource. As the fastest-growing plant on the planet, its carbon-rich lignocellulosic structure is ideal for developing the porosity required for effective adsorption. Specifically, *Schizostachyum brachycladum*, locally known as Lemang bamboo, is widely available in Malaysia, yet much of its biowaste is currently burned or disposed of, contributing to greenhouse gas emissions [2]. The treatment of wastewater containing organic contaminants, particularly synthetic dyes like Methylene Blue, remains a critical environmental challenge. Conventional treatment methods, such as activated sludge or chlorination, are often insufficient for complete dye mineralisation and can lead to secondary contamination. Although activated carbon is a leading adsorbent due to its high surface area, its production from coal involves

significant non-renewable energy consumption and carbon footprints. Furthermore, while chemical activation of biomass using agents like KOH yields high porosity, it generates corrosive alkaline wastewater, posing disposal risks. Conversely, physical activation using steam at high temperatures enhances pollutant diffusion by developing mesopores and macropores without the use of hazardous chemicals [3].

Optimising the performance of bamboo-derived activated carbon (BAC) also requires addressing physical parameters such as particle size and regenerability. Smaller particles may enhance adsorption kinetics but are prone to structural degradation. whereas larger particles offer mechanical stability at the cost of active site accessibility. Moreover, the economic viability of BAC depends on its reusability. Repeated thermal or chemical regeneration cycles can degrade pore structure, necessitating a thorough evaluation of performance loss over time [4]. To address these shortcomings, this research evaluates the development of activated carbon from *Schizostachyum brachycladum* via thermal activation at 750°C using superheated steam. This study investigates the physicochemical properties of the resultant adsorbent, the influence of particle size (1–3 mm) on adsorption capacity, and the efficiency of regeneration protocols, aiming to establish a robust and sustainable solution for wastewater treatment.

2. Materials and Method

2.1 Materials and Equipment

Schizostachyum brachycladum or Lemang bamboo can be obtained easily in Malaysia, it can even be purchased through E-commence platform such as Shoppe. Methylene Blue with 1% aqueous concentration is obtained from material laboratory of University Tun Hussein Onn Malaysia and a stock solution of 1L was prepared by mixing 1.35 ml of Methylene Blue (MB) in 998.65 ml of distilled water. All the working solutions of 0.1%, 0.05% and 0.01% concentration are prepared by serially diluting the stock of MB in 500 ml of distilled water. DR6000 UV-VIS Spectrophotometer, Fourier-Transform Infrared Spectroscopy (FTIR), COXEM EM-30AX Plus SEM-EDX and Bruker D2 Phaser bench-top X-ray diffractometers are the main equipment that are used to characterise bamboo derive activated carbon.

2.2 Bamboo-derived Activated Carbon, BAC Preparation

The collected Lemang bamboo is first wash using tap water to remove any debris or dirt that are stuck on the surface and inside the bamboo. After that, the bamboo is sun dry for several days to remove moisture inside the bamboo. Then, the bamboo is cut into small pieces to be carbonised inside the custom build furnace shown in figure 1. Raw bamboo biomass is subjected to thermal decomposition in an oxygen-deprived environment (pyrolysis). This stage typically occurs at temperatures between 400–600°C. The primary goal of this step is to remove volatile organic compounds (VOCs) and moisture from the bamboo, leaving behind a carbon-rich char with a rudimentary pore structure. The quality of this initial char is critical, as the carbonisation temperature directly influences the distribution of active sites that will be developed in the next stage.

Figure 1: Custom Build furnace for Bamboo Carbonisation

Following carbonisation, the char undergoes physical activation to significantly enhance its surface area and porosity. In this study, the activation is performed using superheated steam at a high temperature of 750°C. This superheated steam acts as an activating agent that "uncorks" the bamboo's inherent vascular structure, gasifying the amorphous carbon and clearing out the pores. This creates a "clean" hierarchical structure containing micro-, meso-, and macropores, which is essential for the effective diffusion and adsorption of larger molecules like MB. The study highlights that this physical activation method is cleaner and more sustainable than chemical activation, as it avoids the generation of corrosive effluent and toxic tar sludge.

2.3 Characterisation of BAC

2.3.1 Adsorption Experiment

The adsorption capability of the BAC was evaluated using MB as a model organic pollutant. A stock solution was prepared by dissolving MB in deionised water to create a 1% aqueous solution. Working solutions for the adsorption tests were subsequently prepared by diluting this stock solution into 500 mL of deionised water to achieve target concentrations with dilution factors of 0.1%, 0.05%, and 0.01%. Batch adsorption experiments were conducted to determine the equilibrium data and adsorption kinetics. A known mass of the BAC (m) was added to 500 mL of the MB solution at the varying initial concentrations described above. The system was allowed to interact until equilibrium was reached to facilitate the understanding of binding mechanisms. After 3 hours of contact times the mixture of AC and MB was filtered using vacuum filter and Whatman filter paper, where the filtrate was used to determine the amount of dye remaining in the solutions and the residue of the Methylene Blue concentrations in the solutions will be analysed using UV-VIS spectrophotometer at 664 nm. The removal efficiency of the pollutant was measured using the percentage of removal, equation (1) and the adsorption capacity, equation (2)

$$R\% = \frac{C_0 - C_e}{C_0} \times 100 \quad (1) \qquad q_e = \frac{(C_0 - C_e)V}{m} \quad (2)$$

where $\mathbf{C_0}$ is an initial concentration, Ce equilibrium concentrations at time “t”, V is the volume of the solution (L) and m is the mass of the AC (g), R% is removal efficiency and qe is adsorption capacity.

2.3.2 Adsorption Isotherms

Adsorption isotherms were developed at equilibrium by manipulating the initial pollutant concentrations to understand the distribution of adsorbate molecules between the liquid and solid phases. The equilibrium data were fitted to two prominent theoretical models, the Langmuir and Freundlich isotherms. The Langmuir isotherm model assumes monolayer adsorption occurs on a structurally homogeneous adsorbent surface, where all binding sites are energetically equivalent and no interaction occurs between adsorbed molecules. This model is often indicative of chemisorption and represented by equation (3).

$$\frac{C_e}{q_e} = \frac{C_e}{q_m} + \frac{1}{q_m K_L} \quad (3)$$

Where Ce is represented as the equilibrium or final concentration of the adsorbate with the unit of mg/L, for qe it is the amount of adsorbate adsorbed per unit mass of adsorbent in mg/g. while qm is represent as the maximum monolayer adsorption capacity which is also calculated in mg/g and KL is the Langmuir constant that related to the free energy pf adsorption in L/mg. The values of qm and KL are obtained from the slope and intercept from the linear graph plot of C_e/q_e. Conversely, the Freundlich isotherm model is an empirical equation describing adsorption on heterogeneous surfaces with a non-uniform distribution of adsorption heat and affinities, often associated with multilayer adsorption, represented by equation (4).

$$log q_e = log K_F + \frac{1}{n} log C_e \quad (4)$$

KF is referred to as the Freundlich constant that indicates the adsorption capacity and 1/n is the adsorption intensity or surface heterogeneity factor. KF and n are obtained from the interception and slope of the graph plot of log qe over log Ce. The n value is used to evaluate the favorability of the adsorption process where the value between 1 to 10 (1<n<10) indicates a favourable adsorption.

2.3.3 Characterisation of BAC

The physicochemical properties of the prepared activated carbon were comprehensively analysed to evaluate its surface morphology, chemical functionality, and crystallographic structure. The characterisation process involved the use of SEM, Fourier-Transform Infrared (FTIR) spectroscopy, and XRD.

2.3.3.1 SEM analysis)

To examine the surface texture and the development of porosity resulting from the activation process, the samples were analysed using SEM. The specific instrument employed for this analysis was the COXEM EM-30AX Plus SEM-EDX machine. This analysis allowed for the visual assessment of the pore formation and structural changes on the carbon surface induced by physical activation. SEM analysis is conducted at University Tun Hussein Onn Malaysia. The samples need to be dried in the oven for 24 hours before being employed for SEM analysis. An aluminium specimen stubs with double side tape is used to attach BAC powder and coated with gold. The imaging is done with a resolution of 10 µm and a guaranteed capacity of 20kV.

2.3.3.2 FTIR analysis

The surface functional groups of the activated carbon were identified using Fourier-Transform Infrared (FTIR) spectroscopy. This technique was utilised to determine the chemical structure, and specific functional groups present on the adsorbent's surface, which play a critical role in the adsorption mechanism. The analysis focused on identifying oxygen-rich functional groups and aromatic ring structures that contribute to the material's adsorption capability. The spectrum of FTIR is recorded at the region of 400-4000 cm-1.

2.3.3.3 XRD

The crystalline and phase composition of the activated carbon were investigated using XRD. The analysis was conducted using a Bruker D2 Phaser bench-top X-ray diffractometer. This method was used to characterise the degree of graphitisation and to detect the presence of any turbostratic disorder within the carbon matrix.

2.3.4 Regeneration and Reusability

To assess the economic viability and sustainable application of the prepared activated carbon, regeneration and reusability studies were conducted. The primary objective was to evaluate the material's ability to recover its adsorption capacity over multiple cycles. The regeneration of the spent activated carbon was attempted using thermal method. The spent activated carbon was subjected to heat treatment in an oven at 450°C for 1hr in a nitrogen atmosphere with the flowrate of 50mL/min. This method aims to volatilise adsorbed organic compounds and decompose pollutants into gaseous by-products, thereby freeing up the active sites.

3. Results and Discussion

3.1 Adsorption Performance

The batch adsorption performance of BAC was evaluated under varying operational conditions, specifically altering the initial MB concentration alongside the adsorbent particle size. The experiments employed a fixed adsorbent dosage of 50 g, a contact time of 60–120 minutes, and a solution pH of 7–8. The resulting removal efficiencies and final concentrations (C_e) are summarised in Table 1

Progress in Engineering Application and Technology Vol. 7 No. 1 (2026) p. 597-610

Table 1: Adsorption performance of activated carbon derived from bamboo

Dilution factor for 1% aqueous solution of MB	Initial concentrationC_0	Final concentration,C_e	Removal efficiency (%)
0.1	13.3	10.79	18.85
0.05	6.76	4.53	33.03
0.01	3.19	0.2	85.2

As illustrated in the data, the removal efficiency exhibited a significant increase as the initial concentration decreased and particle size increased. The Granular Activated Carbon (GAC), tested at the lowest concentration of 0.01%, achieved the highest removal efficiency of 85.2%. This was followed by Coarse Activated Carbon (CAC) at a 0.05% concentration with 33.03% removal, and finally, Powdered Activated Carbon (PAC) at a 0.1% concentration, which demonstrated the lowest efficiency at 18.85%. The experimental results present a deviation from standard theoretical expectations regarding particle size. Theoretically, PAC is expected to demonstrate superior and faster adsorption capacity compared to granular forms. This is attributed to the massive external surface area of fine powders and the shortened diffusion path, which minimises resistance for the adsorbate to penetrate the pores [5]. Conversely, GAC typically exhibits slower adsorption rates due to larger particle sizes, which increase the diffusion distance and potential pore blockage, often limiting pollutant access to the internal surface area. However, in this study, GAC outperformed PAC significantly. This inversion of theoretical trends can be attributed to two primary factors, concentration gradient and ash content and pore blockage. For concentrations gradient the GAC was utilised to treat the lowest concentration of MB (0.01%). The lower ratio of pollutant molecules to available active sites likely facilitated higher percentage removal compared to the high-concentration environment (0.1%) subjected to the PAC. Meanwhile in ash content and pore blockage situations the reduced efficiency of the PAC suggests the presence of residual ash or inorganic impurities. High ash content in PAC can obstruct the pore structure, thereby increasing resistance to diffusion and rendering active sites inaccessible. It is posited that the GAC samples produced less ash residue during activation, allowing for a more efficient diffusion rate [6] [7].

3.2 Adsorption Isotherm

The evaluation of adsorption isotherms is a critical component in understanding the equilibrium relationship between the adsorbate concentration in the liquid phase and the amount adsorbed on the solid surface at a constant temperature. In this study, the adsorption behaviour of MB onto BAC was rigorously analysed using two standard empirical models, the Langmuir and Freundlich isotherms which is shown in figure 2 and 3. These models are essential for elucidating the nature of the adsorption process, specifically distinguishing between monolayer adsorption on a homogeneous surface and multilayer adsorption on a heterogeneous surface [8]. The accurate fitting of these models to the experimental data allows for the determination of key physicochemical parameters that define the efficiency and capacity of the adsorbent.

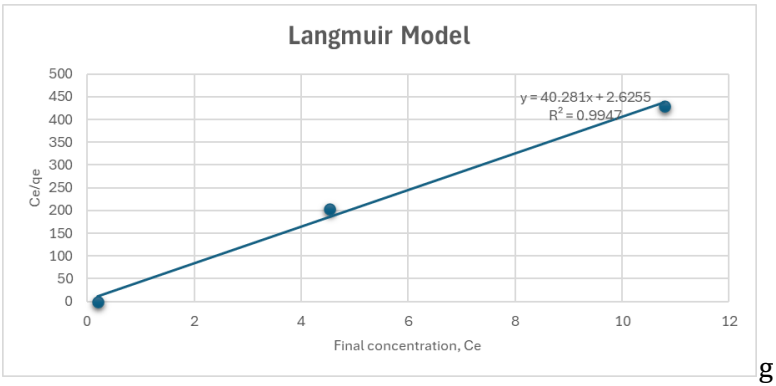

Figure 2: Langmuir isotherm model for adsorption of MB from synthetic wastewater

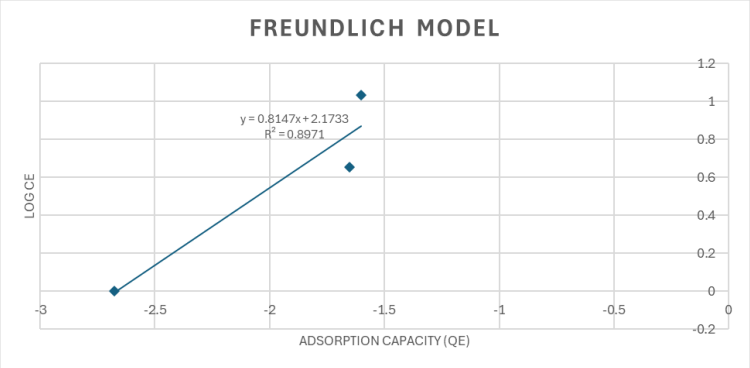

Figure 3: Freundlich isotherm model for adsorption of MB from synthetic wastewater

The statistical analysis of the experimental data demonstrated a distinct conformity to the Langmuir isotherm model over the Freundlich model. The coefficient of determination $\boldsymbol{R^2}$ for the Langmuir model was calculated to be 0.9988, which is significantly higher than the $\boldsymbol{R^2}$ value of 0.8971 obtained for the Freundlich model. This statistical superiority indicates that the adsorption of MB onto the BAC is best described by the Langmuir equation, implying that the process is characterised by monolayer adsorption. This suggests that the adsorption occurs at specific homogeneous sites within the adsorbent, and once a dye molecule occupies a site, no further adsorption can take place at that location, effectively limiting the formation of multilayers. Further examination of the Langmuir constants provides deeper insight into the affinity and binding strength of the adsorption system [9]. The study reported a Langmuir constant $\boldsymbol{K_L}$ of 1.72, a parameter that reflects the energy of adsorption. A high $\boldsymbol{K_L}$ value is indicative of a strong binding affinity between the adsorbate molecules and the adsorbent surface, suggesting that the BAC exhibits a robust capacity for retaining MB ions from the aqueous solution.

Additionally, the maximum monolayer adsorption capacity ($\boldsymbol{q_{max}}$) derived from the model was found to be 0.026243, quantifying the theoretical limit of the adsorbent's performance under the specific experimental conditions. While the Langmuir model provided the optimal fit, the parameters derived from the Freundlich model also offered valuable data regarding the adsorption intensity. The Freundlich heterogeneity factor, *n*, was calculated to be 1.23. In the context of adsorption kinetics and thermodynamics, a value of *n* greater than unity (n > 1) is generally associated with favourable physical adsorption conditions [10]. Although the lower correlation coefficient suggests the surface is not predominantly heterogeneous, the derived values confirm that the adsorption process is favourable. Collectively, these isotherm results validate the potential of BAC as a highly effective, homogeneous adsorbent for the remediation of wastewater containing synthetic dyes.

3.3 SEM

The utilization of Scanning Electron Microscopy (SEM) is pivotal in elucidating the surface topography and textural evolution of activated carbon (AC), particularly in assessing the efficacy of activation protocols. In the context of adsorption science, the efficiency of an adsorbent is fundamentally governed by its physicochemical architecture, where Specific Surface Area (SSA) and pore size distribution play critical roles [11]. High-resolution imaging reveals that the structural hierarchy comprising micropores, mesopores, and macropores is essential for facilitating the kinetic transport and selective sorption of target molecules such as methylene blue [12][13]. Consequently, the morphological analysis serves as a direct indicator of the material's potential for environmental remediation applications.

The SEM analysis of the Lemang bamboo (*Schizostachyum brachycladum*) activated carbon synthesized in this study exhibits a highly ordered, honeycomb-like arrangement of pores, which is identified as the structural fingerprint of the bamboo precursor [13]. Remarkably, the investigation demonstrates that the lignocellulosic framework of the bamboo possesses significant thermal stability; even after undergoing carbonization at temperatures exceeding 700°C, the material retains its characteristic vascular bundles. This retention of the precursor's natural vascular structure is instrumental in the formation of a robust porous network, which is a prerequisite for high-performance adsorption [14]

A critical finding from the surface morphology analysis is the prevalence of macropores with diameters ranging from approximately 2 to 10 µm. These large pores are strategically significant as they function as feeder channels, reducing diffusional resistance and facilitating the mass transfer of adsorbate molecules into the deeper

Progress in Engineering Application and Technology Vol. 7 No. 1 (2026) p. 597-610

internal microporous structure [15]. The presence of such macropores is particularly advantageous for the adsorption of larger organic dye molecules, as they ensure easy accessibility to the active sites located within the carbon matrix. This hierarchical pore architecture, characterized by the coexistence of distinct pore sizes, underscores the effectiveness of the superheated steam activation method in developing a material with superior adsorptive capacities [16][17].

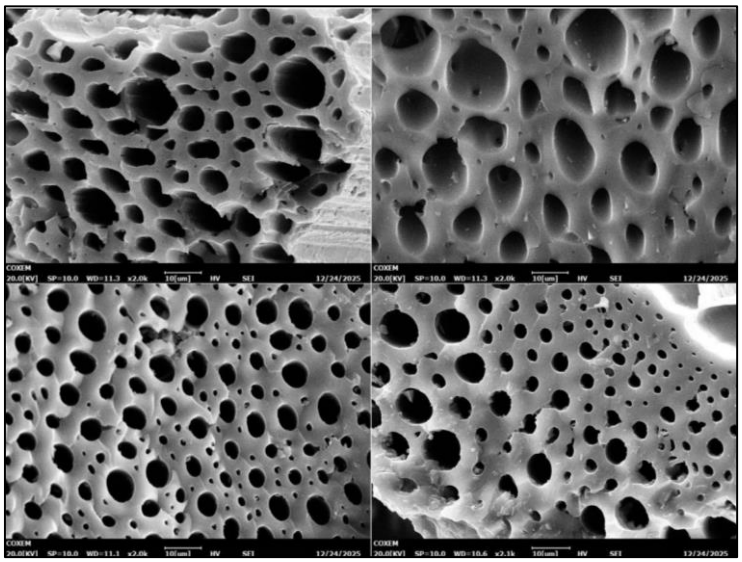

Figure 4: SEM micrograph of BAC at

3.4 FTIR

Fourier-Transform Infrared (FTIR) spectroscopy analysis of the prepared BAC reveals critical insights into the transformation of the lignocellulosic precursor into a functionalised porous material. The precise assignment of spectral bands is fundamental for elucidating the impact of thermal activation and carbonisation on the development of surface oxygenated functional groups (OFGs), which are pivotal for applications in environmental remediation. This spectroscopic characterisation bridges the understanding of the raw biomass's chemical composition and the resulting activated carbon's structural properties, providing a molecular-level roadmap that correlates activation parameters with surface chemistry modifications.

In the high-frequency region of the spectrum, the physical form of the activated carbon, whether powdered or granular, distinctly influences the vibrational characteristics of surface functional groups. As indicated in figure 5 below the spectra for powdered and granule BAC exhibit prominent absorption peaks at 3347.09 cm^{-1} and 3173 cm^{-1}, respectively, which are characteristic of O-H stretching vibrations. These bands are attributed to hydroxyl functional groups present in phenolic and alcoholic structures, as well as physical surface-bound water molecules entrapped within the porous matrix. Furthermore, the intensity of these peaks signifies the presence of intermolecular hydrogen bonding between functional groups, underscoring the complex surface interactions inherent in the material [18].

Conversely, the coarse BAC demonstrates a spectral shift with a lower frequency feature observed at 3061 cm^{-1}, suggesting a divergence in structural evolution during the activation process. This specific wavenumber is associated with aromatic ring structures or aliphatic C–H stretching vibrations, indicating the presence of hydrogen atoms located at the edges of graphitic crystallites or within aliphatic chains bound to the carbon skeleton. Such spectral evidence points to the formation of a more condensed aromatic matrix, which is a key indicator of the material's carbonisation degree and structural stability [19].

The analysis of the fingerprint region, particularly between 1550 cm^{-1} and 1600 cm^{-1}, further corroborates the development of a graphitic carbon backbone. Intense peaks observed at 1573.27 cm^{-1} for powdered, 1582.05 cm^{-1} for granule, and 1572 cm^{-1} for coarse samples correspond to the skeletal C=C bonds of aromatic rings. These bands serve as major markers for the graphitic carbon skeleton formed during carbonisation. Notably, the peak at 1582.05 cm^{-1} in the granule BAC is also indicative of C=O functionality, revealing the presence of quinone or

ketone groups conjugated with the aromatic system and reflecting the extent of graphitisation and condensation induced by the activation treatment [20].

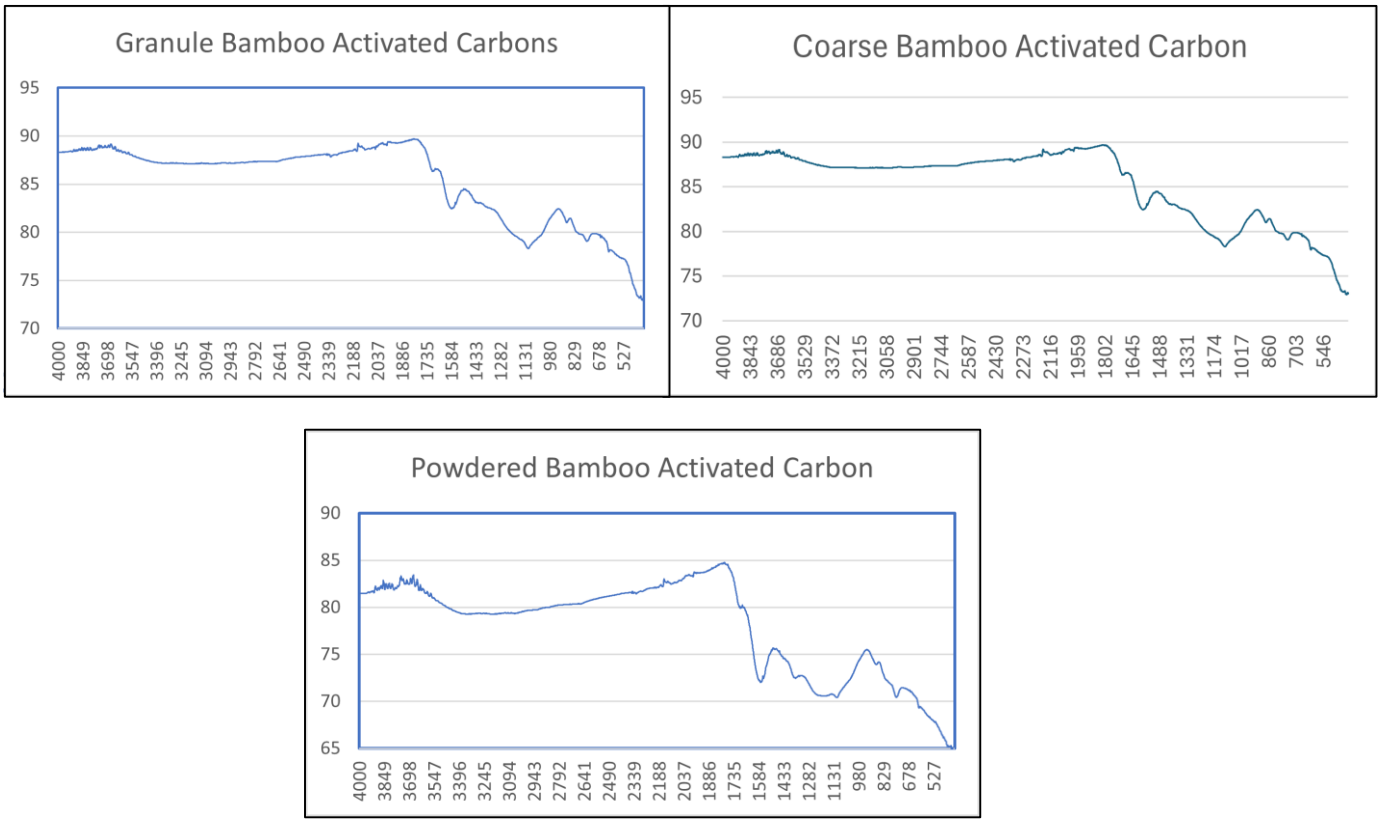

Figure 5: FTIR spectrum of BAC

3.6 X-ray Diffraction

The XRD profile of the Lemang BAC exhibits a distinctive structural architecture that fundamentally diverges from the highly ordered lattice of crystalline graphite as shown in figure 6 below. The diffractogram is characterised principally by broad, diffuse peaks centred at approximately 23-25˚ and 43˚ 2Θ, which constitute the definitive crystallographic signature of turbostratic disorder. In contrast to the sharp diffraction lines that signify the perfect AB stacking inherent to crystalline graphite, this observed pattern indicates a microstructure composed of small stacks of graphene layers. These layers display random rotational and translational misalignments along the c-axis, a phenomenon characteristic of non-graphitising carbons produced at lower carbonisation temperatures [21]. A detailed crystallographic assignment of these peaks provides critical insights into the dimensions of the carbon crystallites. The relatively sharper peak observed at the (002) plane (23-25˚) corresponds to the average inter-layer spacing (d_{002}) and the stacking height (L_c) of the coherent carbon domains, while the broader reflection at the (100) plane (43˚) is associated with the lateral size (L_a) and the degree of in-plane disorder within the graphene sheets [22].

This structural configuration is consistent with observations for biomass and agricultural waste-derived carbons, which typically exhibit significantly higher turbostratic disorder and lower degrees of graphitisation compared to fossil-based carbons. The activation process is instrumental in defining this structure; chemical activation utilising agents such as KOH or H_3PO_4 is particularly effective in maintaining the high level of porosity and the turbostratic framework necessary for optimal adsorption performance [23][24]. Furthermore, the XRD analysis highlights the necessity of distinguishing intrinsic carbon features from mineral impurities retained from the precursor material. Peaks located near 20.8˚ and 26.6˚ are frequently ascribed to quartz silica impurities; however, recent literature suggests that diffraction data alone may be insufficient to confirm these assignments definitively. The presence of such impurities, particularly silica, can have complex implications for the material's properties. While silica may contribute to thermal stability, it has been observed to restrict the formation of an optimal pore structure, thereby potentially limiting the material's adsorption capacity [25][26]. Consequently, to resolve ambiguities in the diffraction data and achieve a complete physicochemical profile, standard protocols

Progress in Engineering Application and Technology Vol. 7 No. 1 (2026) p. 597-610

recommend a multi-analytical approach that integrates XRD with Fourier-Transform Infrared (FTIR) spectroscopy, SEM-EDX, and thermal analysis.

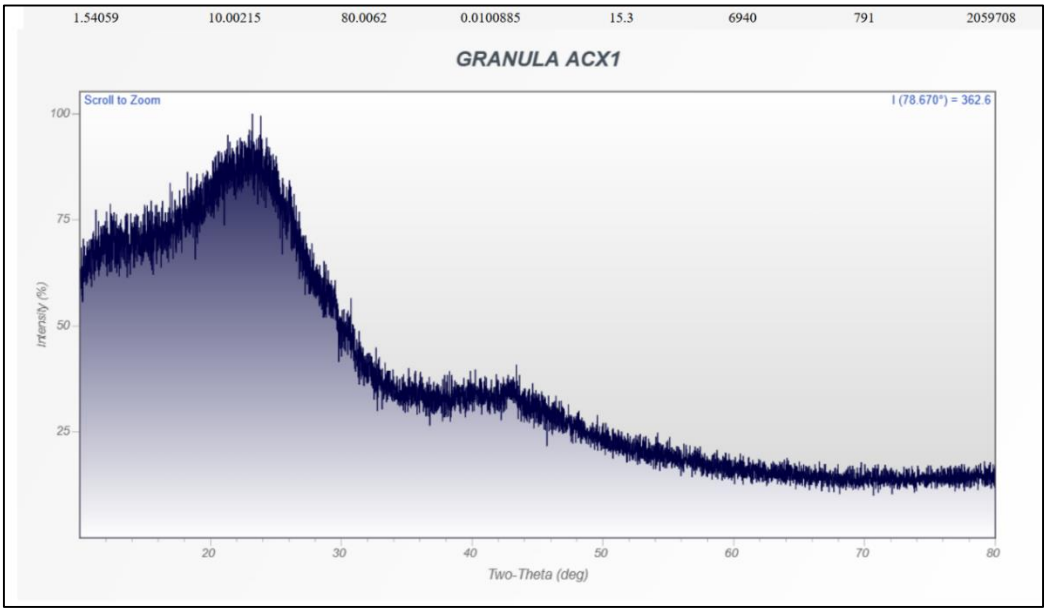

Figure 6: X-ray Diffraction of BAC

3.7 Regeneration and Reusability

The purpose of regeneration and reusability experiment is to identify whether the spent activated carbon can be used again after several adsorption cycles. Through this experiment the recovery of adsorption capacity can be maximised. The regeneration and reusability of bamboo-derived activated carbon cannot be done due to the final concentration (C_e) of regenerated BAC is higher than initial concentration (C_o). Table 2 shows C_e and C_o of the regenerated BAC and the absorbance obtained by using UV-vis. The reason why C_e is higher than C_o is due to the incomplete removal of adsorbed contaminants during regeneration that lead to the elevated C_e. This situation is commonly referred to as "heel". Due to the formation of heel, the pores of the AC became block with the contaminant from previous cycle, thus hindering the regeneration process [27]. When using this imperfect regenerated AC for new adsorption cycle instead of absorbing the MB it will release the old contaminants as well as ash residue inside it. Thus, it will further pollute the water instead of cleaning it which results in higher final concentration.

Table 2: regeneration data of BAC

Initial absorbance C_o	Initial concentration	Absorbance of regenerated AC	Final concentration, C_e
0.221	13.3	0.238	13.53
0.157	6.76	0.08	2.99
0.083	1.35	0.075	2.66

4 Conclusion

The activation of carbon from Schizostachyum brachycladum ("Lemang" bamboo) via physical activation with superheated steam is a highly efficacious and sustainable technique for creating a hierarchical micro-mesoporous carbon with a "clean" structure perfectly suited for larger molecule diffusion and adsorption, such as that of MB adsorbates. The two-stage process entails a carbonisation activation at temperatures ranging from 750°C to 950°C and is typically accomplished via carbonisation followed by activation; this enables the gasification of amorphous carbon and liberation of volatiles sufficient enough to "uncork" the bamboo's inherent vascular structure with a clearly delineated hierarchical micro-mesoporosity pattern.

Unlike traditional methods involving chemical activation with consequent corrosive effluent water generation and production of toxic tar sludge precipitates, superheated water vapour sublation results in a "clean" structure devoid of such tar precipitates without interfering with inherent hierarchical porosities along with a perfectly optimised carbon matrix for enhanced adsorbate diffusion and adsorption along green and sustainable principles with respect to non-toxic waste inputs for a carbon matrix critically suited for sustainable utilisation as a specialised filtering material.

Acknowledgement

The author would like to express thank you towards the Faculty of Engineering Technology, Universiti Tun Hussein Onn Malaysia.

References

[1] Divya, M. P., Krishnamoorthi, S., Ravi, R., Jenner, V. G., Baranidharan, K., Raveendran, M., & Hemalatha, P. (2025). Preparation and characterization of activated carbon from commercially important bamboo species in northeastern India. *Advances in Bamboo Science*, *11*, 100148. https://doi.org/10.1016/j.bamboo.2025.100148

[2] Harimisa, G. E., Jusoh, N. W. C., Tan, L. S., & Ghafar, N. A. (2023). Influence of furnace atmospheres and potassium hydroxide activation on the properties of bamboo activated carbon and its adsorption towards 4-nitrophenol. *Chemical Engineering Research and Design*, *198*, 325–339. https://doi.org/10.1016/j.cherd.2023.09.008

[3] Goh, S. M. X., Chin, B. L. F., Huang, M. M., Yiin, C. L., Kurnia, J. C., Lam, S. S., Tan, Y. H., Chai, Y. H., & Rashidi, N. A. (2024). Harnessing bamboo waste for high-performance supercapacitors: A comprehensive review of activation methods and applications. *Journal of Energy Storage*, *105*, 114613. https://doi.org/10.1016/j.est.2024.114613

[4] Kong, Z., Zhang, H., Zhou, T., Xie, L., Wang, B., & Jiang, X. (2025). Biomass-derived functional materials: Preparation, functionalization, and applications in adsorption and catalytic separation of carbon dioxide and other atmospheric pollutants. *Separation and Purification Technology*, *354*, 129099. https://doi.org/10.1016/j.seppur.2024.129099

[5] Kebede, M. M., Masud, A., Ortbal, S., Shin, W. S., Mekonnen, M. M., Clement, T. P., & Terry, L. G. (2025). Adsorptive Removal of PFAS from Aqueous Solutions Using GAC, PAC and Ball-Milled Colloidal Activated Carbon: Characterizing Efficiency, Kinetics, and Mechanisms. *ACS ES&T Water*, *5*(11), 6554–6566. https://doi.org/10.1021/acsestwater.5c00641

[6] Cárdenas-Piñeros, D. E., Reynel-Ávila, H. E., Díaz-Muñoz, L. L., Bonilla-Petriciolet, A., Durán-Valle, C. J., & Adame-Pereira, M. (2025). Purification of Biodiesel Polluted by Copper Using an Activated

Carbon Prepared from Spent Coffee Grounds: Adsorption Property Tailoring, Batch and Packed-Bed Studies. *Molecules*, *30*(3), 483. https://doi.org/10.3390/molecules30030483

[7] Hwang, S. Y., Lee, G. B., Kim, J. H., Hong, B. U., & Park, J. E. (2020). Pre-Treatment Methods for Regeneration of Spent Activated Carbon. *Molecules*, *25*(19), 4561. https://doi.org/10.3390/molecules25194561

[8] Zerhouni, A., Attouti, S., Termoul, M., Benzekri Benallou, M., Bestani, B., & Benderdouche, N. (2024). Comparative study of Safranin O adsorption onto biomass-derived activated carbon and commercial activated carbon: isotherm modeling. *Studies in Engineering and Exact Sciences*, *5*(2), e12244. https://doi.org/10.54021/seesv5n2-799

[9] Nure, J. F., Mengistu, A., Abewaa, M., Angassa, K., Moyo, W., Phiri, Z., Mafa, P. J., Kuvarega, A. T., & Nkambule, T. T. I. (2023). Adsorption of Black MNN reactive dye from tannery wastewater using activated carbon of Rumex Abysinicus. *Journal of the Taiwan Institute of Chemical Engineers*, *151*, 105138. https://doi.org/10.1016/j.jtice.2023.105138

[10] Dimbo, D., Abewaa, M., Adino, E., Mengistu, A., Takele, T., Oro, A., & Rangaraju, M. (2024). Methylene blue adsorption from aqueous solution using activated carbon of spathodea campanulata. *Results in Engineering*, *21*, 101910. https://doi.org/10.1016/j.rineng.2024.101910

[11] Abbas, A., Ahmed, M., Yousaf, M., Ahmad, R., Afzal, S., & Xu, D. (2025). Engineered biochar from lignocellulosic biomass: Structure-property guided design for targeted contaminant removal in wastewater. *Journal of Molecular Liquids*, *439*. https://doi.org/10.1016/j.molliq.2025.128688

[12] Shi, W., Guo, Y., Lu, Q., Li, H., Liang, Y., Ma, F., Yang, B., & Chang, B. (2025). Dynamic tailoring of the gradient porosity of biomass-derived porous carbons for highly effective CO2 capture. *Green Chemistry*, *27*(37), 11416–11428. https://doi.org/10.1039/d5gc03217b

[13] Wang, B., Xie, Q., Sha, Y., Liu, J., & Liang, D. (2025). Research progress on the preparation of bamboo-based activated carbon for CO_2 adsorption. *New Carbon Materials*, *40*(2), 317–332. https://doi.org/10.1016/s1872-5805(25)60956-5

[14] Li, C., Zhang, J., Gao, B., Guo, Y., Jiang, Y., Fan, M., Wei, T., Zhang, S., & Hu, X. (2025). Contribution of hemicellulose/cellulose to structural evolution of char from pyrolysis, hydrothermal carbonization, gasification and activation of poplar wood. *Journal of Environmental Chemical Engineering*, *13*(6). https://doi.org/10.1016/j.jece.2025.120281

[15] Huang, A., Liu, Z., Yang, S., Lu, X., Wang, S., Wang, Z., & Wu, N. (2026). Removal of H2PO4– in water by forestry waste biochar: Preparation, characteristics, adsorption performance, and mechanism. *Chemical Engineering Journal Advances*, *25*. https://doi.org/10.1016/j.ceja.2025.100973

[16] Mohite, V. S., Patil, P. D., Pawar, S. D., Patil, S. M., & Patil, S. A. (2025). Optimization of dye adsorption by bamboo activated carbon using Taguchi approach. *Desalination and Water Treatment*, *324*. https://doi.org/10.1016/j.dwt.2025.101545

[17] Derkacheva, O. Y., Ponomarev, D. A., Spitsyn, A. A., & Ng'i, C. K. (2021). Change in the Functional Composition of the Carbon Surface upon Water Vapor Activation. *Russian Journal of Applied Chemistry*, *94*(7), 996–1001. https://doi.org/10.1134/S1070427221070181

[18] Di, H., Zhang, T., Ma, H., Zhang, G., Li, K., Han, J., & Yang, J. (2025). Biomass tar modified biochar with enhanced micropores and oxygen content for high efficiency CO_2 capture. *Separation and Purification Technology*, *378*. https://doi.org/10.1016/j.seppur.2025.134678

[19] Isah, U. A., Rashid, M. I., Lee, S., Kiman, S., & Iyodo, H. M. (2024). Correlations of coal rank with the derived Fourier Transform Infra-Red (FTIR) spectroscopy structural parameters: A review. *Infrared Physics & Technology*, *141*, 105456. https://doi.org/10.1016/j.infrared.2024.105456

[20] Hashim, D., Liew, J. Y., Boon, J. G., & Ch'ng, H. Y. (2022). Multipurpose applications of bamboo as an activated carbon: An overview. *Journal of Applied and Natural Science*, *14*(2), 522–530. https://doi.org/10.31018/jans.v14i2.3406

[21] Fujimoto, H. (2003). Theoretical X-ray scattering intensity of carbons with turbostratic stacking and AB stacking structures. *Carbon*, *41*(8), 1585–1592. https://doi.org/10.1016/s0008-6223(03)00116-7

[22] A.G. Fazlitdinova, & V.A. Tyumentsev. (2022). Structural transformations of graphite during dispersion. *Челябинский физико-математический журнал*, *7*(3), 374–383. https://doi.org/10.47475/2500-0101-2022-17311

[23] Yavuz, B., Korkmaz, A. A., Kaya, H., Seher Güler, & Funda Ersoy Atalay. (2025). Preparation and characterization of activated carbon from tomato, pepper, and eggplant wastes by two-step KOH activation. *Chemical Engineering Communications*, *213*(2), 251–263. https://doi.org/10.1080/00986445.2025.2540910

[24] Qi, G., Wei, X., & Junli, L. (2022). Preparation and Electrochemical Performance of Lignin-based Activated Carbon by Phosphoric Acid Activation [磷酸法木质素基活性炭的制备及其电化学性能研究]. *Chemistry and Industry of Forest Products*, *42*(2), 31–38. https://doi.org/10.3969/j.issn.0253-2417.2022.02.005

[25] Xu, W., Liu, J., Sun, K., Liu, Y., Chen, C., Wang, A., & Sun, H. (2021). Effect of activation temperature on properties of H3PO4-activated carbon. *BioResources*, *16*(2), 4007–4020. https://doi.org/10.15376/biores.16.2.4007-4020

[26] Zhao, C., Ge, L., Mai, L. P., Li, X., Chen, S., Li, Q., Li, S., Yao, L., Wang, Y., & Xu, C. (2023). *Review on Coal-Based Activated Carbon: Preparation, Modification, Application, Regeneration, and Perspectives*. https://doi.org/10.1021/acs.energyfuels.3c01866

[27] Weiye, Z., Jing, S., Yipeng, S., Huaigang, C., & Huirong, Z. (2025). Analysis of heel formation and influencing factors during the thermal regeneration process of saturated activated carbon [饱和活性炭热再生过程残余物形成及影响因素分析]. *Industrial Water Treatment*, *45*(1), 17–25. https://doi.org/10.19965/j.cnki.iwt.2024-0156